Title

Context-dependent modulation of Pol II CTD phosphatase SSUP-72 regulates alternative polyadenylation in neuronal development

Journal

Genes & Development, 29(22)

ISSN

0890-9369

Authors

Chen, Fei
Zhou, Yu
Qi, Yingchuan B
et al.

Publication Date

2015-11-15

DOI

10.1101/gad.266650.115

Peer reviewed

Context-dependent modulation of Pol II CTD phosphatase SSUP-72 regulates alternative polyadenylation in neuronal development

Fei Chen,[1,2] Yu Zhou,[3] Yingchuan B. Qi,[1,6] Vishal Khivansara,[4,7] Hairi Li,[3] Sang Young Chun,[5] John K. Kim,[4,8] Xiang-Dong Fu,[3] and Yishi Jin[1,2,3]

[1]Neurobiology Section, Division of Biological Sciences, University of California at San Diego, La Jolla, California 92093, USA; [2]Howard Hughes Medical Institute, University of California at San Diego, La Jolla, California 92093, USA; [3]Department of Cellular and Molecular Medicine, School of Medicine, University of California at San Diego, La Jolla, California 92093, USA; [4]Life Sciences Institute, Department of Human Genetics, University of Michigan, Ann Arbor, Michigan 48109, USA; [5]Department of Computational Medicine and Bioinformatics, University of Michigan, Ann Arbor, Michigan 48109, USA

Alternative polyadenylation (APA) is widespread in neuronal development and activity-mediated neural plasticity. However, the underlying molecular mechanisms are largely unknown. We used systematic genetic studies and genome-wide surveys of the transcriptional landscape to identify a context-dependent regulatory pathway controlling APA in the *Caenorhabditis elegans* nervous system. Loss of function in *ssup-72*, a Ser5 phosphatase for the RNA polymerase II (Pol II) C-terminal domain (CTD), dampens transcription termination at a strong intronic polyadenylation site (PAS) in *unc-44/ankyrin* yet promotes termination at the weak intronic PAS of the MAP kinase *dlk-1*. A nuclear protein, SYDN-1, which regulates neuronal development, antagonizes the function of SSUP-72 and several nuclear polyadenylation factors. This regulatory pathway allows the production of a neuron-specific isoform of *unc-44* and an inhibitory isoform of *dlk-1*. Dysregulation of the *unc-44* and *dlk-1* mRNA isoforms in *sydn-1* mutants impairs neuronal development. Deleting the intronic PAS of *unc-44* results in increased pre-mRNA processing of neuronal ankyrin and suppresses *sydn-1* mutants. These results reveal a mechanism by which regulation of CTD phosphorylation controls coding region APA in the nervous system.

[*Keywords*: pre-mRNA 3′ end processing; axon and synapse development; *C. elegans*; SYDN-1; UNC-44/ankyrin; DLK-1/MAP kinase]

Supplemental material is available for this article.

Received June 1, 2015; revised version accepted October 16, 2015.

Alternative polyadenylation (APA) occurs at polyadenylation [poly(A)] sites (PASs) residing within the 3′ untranslated region (UTR) or in internal introns/exons. mRNAs with long 3′ UTRs generally contain regulatory elements that affect mRNA stability, localization, and translation efficiency. mRNA isoforms with different coding exons produce protein variants that often have distinct or opposing functions (Di Giammartino et al. 2011). Over 50% of human genes have multiple PASs (Tian et al. 2005). Tissue- and gene-specific APA events are widespread in normal and pathological conditions (Elkon et al. 2013). For example, rapidly dividing cells or cancer cells preferentially use proximal PASs to produce mRNAs with shorter 3′ UTRs than differentiated cells (Sandberg et al. 2008; Mayr and Bartel 2009). In addition, genes with tissue-restricted expression often have single 3′ UTRs, while ubiquitiously transcribed genes generate multiple 3′ UTRs and may use different 3′ UTR isoform ratios to achieve tissue-specific expression (Lianoglou et al. 2013).

Nuclear polyadenylation (NpolyA) produces the 3′ UTRs of mature mRNAs and involves four major subcomplexes (Colgan and Manley 1997; Millevoi and Vagner 2010; Proudfoot 2011). Cleavage and polyadenylation specificity factors (CPSFs) bind to PASs, which predominantly consist of the AAUAAA hexamer; cleavage stimulation

Present addresses: [6]Institute of Developmental and Regenerative Biology, School of Life and Environmental Sciences, Hangzhou Normal University, 310036 Hangzhou, China; [7]Children's Research Institute, Department of Pediatrics, University of Texas Southwestern Medical Center, Dallas, TX 75390, USA; [8]Department of Biology, Johns Hopkins University, Baltimore, MD 21218, USA.
Corresponding author: yijin@ucsd.edu
Article is online at http://www.genesdev.org/cgi/doi/10.1101/gad.266650.115.

factors (CstFs) bind to U/GU-rich regions downstream from the cleavage site; and cleavage factors (CFI and CFII) bind to a UGUA motif upstream of the cleavage site. Together with poly(A) polymerase, these complexes coordinate the recognition of *cis* elements in the 3′ UTRs of pre-mRNA and execute pre-mRNA cleavage and addition of polyadenine. While differential expression of NpolyA core factors or 3′ UTR-binding proteins has been linked to cell type- and tissue-specific APA within 3′ UTRs (Licatalosi et al. 2008; Kim et al. 2010b; Hilgers et al. 2012; Jenal et al. 2012; Martin et al. 2012; Masamha et al. 2014), much less is known about how APA at internal intronic/exonic PASs is regulated. During B-cell differentiation, up-regulation of the polyadenylation factor CstF-64 leads to usage of intronic PASs (Takagaki et al. 1996). U1 small nuclear ribonucleoproteins (snRNPs) can prevent premature cleavage and polyadenylation in a splicing-independent manner (Kaida et al. 2010). In neurons, depolarization triggers a transient shortage of U1 snRNPs and prompts the use of internal or proximal PASs (Flavell et al. 2008; Berg et al. 2012).

The C-terminal domain (CTD) of the large subunit of RNA polymerase II (Pol II) is a key regulator of the NpolyA machinery (McCracken et al. 1997; Hirose and Manley 1998). In eukaryotic cells, the CTD consists of 26–52 repeats of the heptapeptide YSPTSPS. The phosphorylation state of each Ser in the heptapeptide has been proposed to function as a "CTD code" that regulates transcription initiation, elongation, and termination (Egloff and Murphy 2008; Buratowski 2009). In particular, Ser2 phosphorylation of the CTD is required for its association with polyadenylation factors in 3′ end formation of pre-mRNA (Hirose and Manley 1998; Licatalosi et al. 2002; Ahn et al. 2004; Meinhart and Cramer 2004; Davidson et al. 2014). Multiple kinases and phosphatases are involved in CTD phosphorylation and dephosphorylation (Meinhart et al. 2005). Among them, the Ssu72 family of phosphatases primarily dephosphorylates Ser5 (Sun and Hampsey 1996; Krishnamurthy et al. 2004). Structural studies show that Ssu72 directly binds the CTD heptapeptide and forms a complex with symplekin (Xiang et al. 2010), a component of the CPSF complex (Kolev et al. 2008; Sullivan et al. 2009). Biochemical studies show that this complex regulates transcription-coupled polyadenylation (Xiang et al. 2010). Yeast Ssu72, the founding member of the family, is essential (Sun and Hampsey 1996). Mammalian Ssu72 is highly expressed in the brain (St-Pierre et al. 2005), but its in vivo function is unknown.

In the nematode *Caenorhabditis elegans*, most of the conserved components of the NpolyA machinery are essential for embryonic and larval development (Cui et al. 2008). Their roles in the nervous system are largely unknown. The novel nuclear protein SYDN-1 was previously discovered in a genetic enhancer screen for synapse formation and was subsequently shown to negatively regulate *pfs-2* (Van Epps et al. 2010), the ortholog of human WDR33, an obligatory subunit of the CPSF complex that binds the AAUAAA hexamer (Chan et al. 2014; Schonemann et al. 2014). While the genetic evidence indicates that SYDN-1 inhibits NpolyA activity, it is not known which step of NpolyA and what genes regulated by SYDN-1 are critical for neuronal development.

Here, we identify SSUP-72, the *C. elegans* ortholog of Ssu72, through analyses of genetic suppressors of *sydn-1* mutants. SYDN-1 can bind SSUP-72 and interfere with its association with RNA Pol II. By analyzing the genomic occupancy of Pol II CTD in combination with transgenic reporter assays, we uncovered that SSUP-72 regulates APA at coding region PASs. The interaction of SYDN-1 and SSUP-72 is necessary for the production of the neuron-specific isoform of the ankyrin protein UNC-44 and an inhibitory isoform of the MAPKKK DLK-1. We show that the strength of intronic PASs in *unc-44* and *dlk-1* plays distinct roles for 3′ end processing and transcription termination. Dysregulation of APA of *unc-44* or *dlk-1* contributes to neuronal defects in *sydn-1* mutants. Furthermore, deletion mutations in the coding region PAS of *unc-44* cause enhanced pre-mRNA processing of the neuronal isoform and suppress *sydn-1* mutants. Taken together, our data reveal a molecular mechanism controlling coding region APA in the nervous system.

Results

Negative regulation of a subset of NpolyA factors by SYDN-1 is required for neuronal development in C. elegans

In a genetic screen for regulators of synapse formation, we previously identified the novel nuclear protein SYDN-1 (Van Epps et al. 2010). *sydn-1(0)*-null mutants exhibit mild behavioral deficits but display strong genetic synergy with other mutants affecting synaptic development. For example, double mutants of *sydn-1(0)* with *syd-2(0)*/α-*liprin* display severe paralysis, diminished synapse number, and excessive axon branching—phenotypes not found in *sydn-1(0)* or *syd-2(0)* single mutants (Van Epps et al. 2010). We took advantage of these synthetic behavioral deficits and isolated a large number of genetic suppressors (Supplemental Material). We characterized multiple mutations that suppressed the synapse and axon morphology defects of *sydn-1(0)* but not of *syd-2(0)* (Fig. 1A–C; Supplemental Fig. S1A). In addition to the previously reported *pfs-2*/WDR33 (Van Epps et al. 2010), we identified three new genes (Figs. 1C, 2A; Supplemental Table S1): *cpsf-4*, which encodes the 30-kDa subunit of the CPSF complex; *zfp-3*, which encodes a novel zinc finger protein that can interact with NpolyA proteins; and *ssup-72*, which encodes the ortholog of CTD Ser5 phosphatase Ssu72. We also tested additional NpolyA genes and found three other genes in which mutations also strongly suppressed *sydn-1 (0)* (Fig. 1C; Supplemental Fig. S1A,B). These included *symk-1*/*symplekin*, a binding partner of Ssu72 and CTD (Xiang et al. 2010), and *cids-1* and *cids-2*, which encode two homologous proteins of the RTT103 family, known to interact with the Ser2 phosphorylated CTD (Kim et al. 2004). In contrast, null or partial loss-of-function alleles of *cpf-1* and *suf-1*, encoding CstF50 and CstF77, respectively, and a null mutation of *nrd-1*, which encodes a protein that can bind the Ser5 phosphorylated CTD

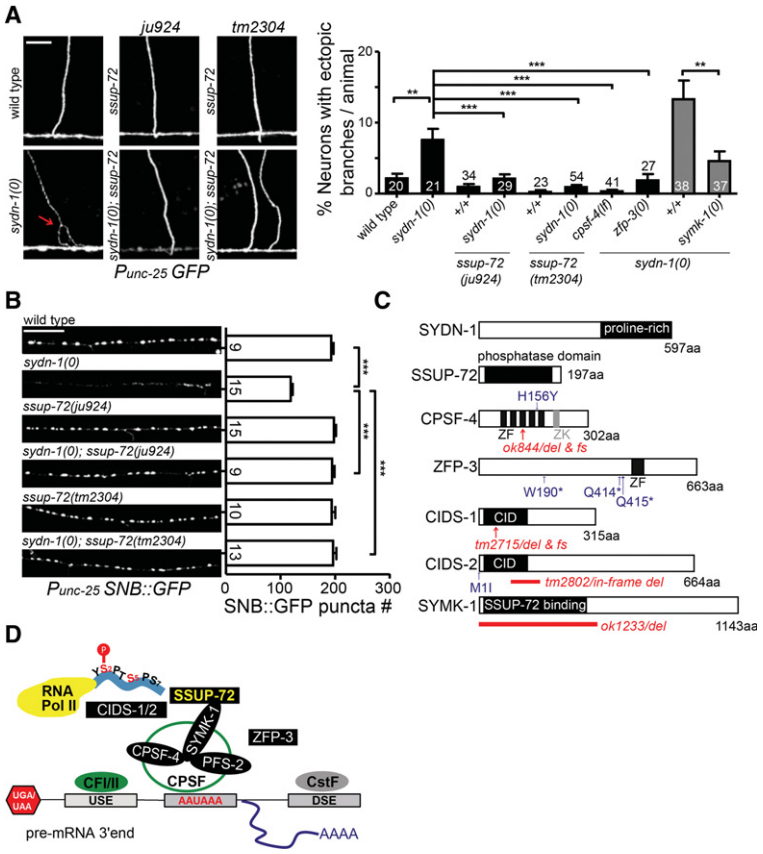

Figure 1. Identification of *ssup-72* and select NpolyA components as suppressors of *sydn-1(0)*. (*A*) Suppression of motor neuron axonal morphology defects in *sydn-1(0)*. Images show axonal morphology of the GABAergic motor neurons labeled by *juIs76 [Punc-25-GFP]*. In *sydn-1(0)* animals, circumferential commissures have ectopic branches (red arrow) and appear thinner than those in wild type or *ssup-72(0)*. Both *ssup-72(0)* alleles (*ju924* and *tm2304*) completely suppress the axon morphology defects in *sydn-1(0)*. The graph at the *right* shows the quantification of suppression. Fifteen to 19 commissures were counted per adult animal (black bars) or five to six commissures per L1 animal (gray bars); data are shown as the average percentage of abnormal neurons per animal (mean ± standard error of the mean [SEM]; *n* = number of animals). (**) $P < 0.01$; (***) $P < 0.001$, Kruskal-Wallis test and Dunn's multiple comparison post-test (black bars); (**) $P < 0.01$, Mann-Whitney test (gray bars). Bar, 10 µm. (*B*) Suppression of motor neuron presynaptic morphology defects in *sydn-1(0)*. Images show synaptic puncta in the dorsal nerve cord of the GABAergic motor neurons labeled by *juIs1 [Punc-25-SNB::GFP]*. *sydn-1(0)* animals show fewer synaptic puncta and larger gaps than those in wild type and *ssup-72(0)*. Both *ssup-72(0)* alleles (*ju924* and *tm2304*) completely suppress the synaptic defects in *sydn-1(0)*. The graph at the *right* shows the quantification of suppression; data are shown as the total synaptic puncta in the dorsal cord (mean ± SEM; *n* = number of animals). (***) $P < 0.001$, Kruskal-Wallis test and Dunn's multiple comparison post-test. Bar, 20 µm. (*C*) Summary of the proteins and mutations identified from the suppressor analysis of *sydn-1(0)*. (ZF) Zinc finger domain; (ZK) zinc knuckle domain; (CID) CTD-interacting domain. The SSUP-72-binding domain of SYMK-1 is predicted based on homology (Xiang et al. 2010). (*D*) Schematic illustration of protein interaction of the *sydn-1(0)* suppressor genes based on reported studies on their homologs. One heptapeptide of RNA Pol II CTD is shown, and Ser2 residue is phosphorylated at the 3′ end of pre-mRNA. (CFI/II) Cleavage factors; (USE) upstream element; (DSE) downstream element; (AAUAAA) canonical poly(A) signal.

(Vasiljeva et al. 2008), did not suppress *sydn-1(0)* (Supplemental Fig. S1A,B; data not shown). Thus, the suppression of the neuronal and behavioral defects in *sydn-1(0)* appears to be highly selective to a subset of the genes in the NpolyA machinery (Fig. 1D).

Single mutants of *sydn-1(0)* suppressors displayed grossly normal axon and synapse morphology and locomotion and behaved as loss of function. For example, *cpsf-4 (ju605)* changes a conserved His156 to Tyr in the fourth zinc finger domain of CPSF-4 (Fig. 1C) and suppresses the motor neuron axon branching defects of *sydn-1(0); syd-2 (0)* animals to the same degree as a null mutation *cpsf-4 (ok844)* (Supplemental Fig. S1A). Neuron-specific expression of *cpsf-4(+)* rescued the suppression of *cpsf-4(lf)* on *sydn-1(0)* (Supplemental Fig. S1C), supporting a cell-autonomous requirement of CPSF-4.

The genetic interaction between *sydn-1* and CPSF components raised the possibility that SYDN-1 might affect PAS recognition and/or utilization in general. To address this, we assessed usage of PASs by deep sequencing 3′ ends of mRNAs prepared from stage-matched wild-type and *sydn-1(0)* animals (Supplemental Material). We obtained comparable numbers of unique reads of 3′ ends from *sydn-1(0)* and wild type (Supplemental Fig. S2A) and found that the overall pattern of PAS usage in *sydn-1(0)* was similar to wild type (Supplemental Fig. S2B). As transcripts from neuronal genes might generally be low in such samples, we also tested multiple neuronal genes by 3′RACE and observed that their PAS usage was not altered in *sydn-1(0)* (Supplemental Figs. S2C, S3). This analysis suggests that SYDN-1 is unlikely to be required for general recognition of PASs. Instead, SYDN-1 may regulate NpolyA of specific neuronal genes. To dissect this pathway, we focused on *ssup-72*, as null mutants of *ssup-72* completely suppress *sydn-1(0)* and are fully viable.

SSUP-72 phosphatase activity is required for its function in SYDN-1-dependent neuronal development

SSUP-72 shares 57% amino acid identity with human Ssu72 (Fig. 2A). The catalytic nucleophile of human Ssu72 consists of residues Cys12 and Asp143 flanking a two-stranded anti-parallel β sheet (β2A and β2B) (Xiang et al. 2010). *ssup-72(ju924)*, isolated as a *sydn-1(0)* suppressor, alters an invariant Gly47 in the loop of the β sheet. A null mutation, *ssup-72(tm2304)*, which deletes most of the coding sequence, suppressed the synaptic and axon defects of *sydn-1(0)* to levels similar to those of *ssup-72(ju924)* (Fig. 1A,B). Genetic mosaic analysis

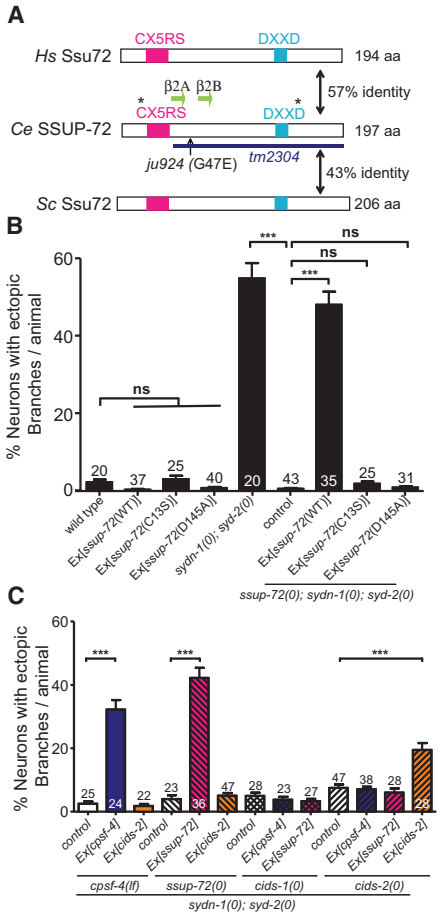

Figure 2. SSUP-72 phosphatase activity is required in the SYDN-1-dependent pathway during neuronal development. (*A*) Illustration of the SSUP-72 family. The catalytic nucleophile (CX_5RS) and aspartate loop (DXXD) are essential for the CTD phosphatase activity. (*B*) Wild-type but not phosphatase mutant *ssup-72* rescues the suppression of *sydn-1(0)* by *ssup-72(0)*. *syd-2(0)* was used to sensitize detection of the suppression. (*C*) The function of the suppressor genes of *sydn-1(0)* is dependent on each other. Transgenes overexpressing *ssup-72*, *cpsf-4*, or *cids-2* cannot bypass the requirement of other suppressor genes. Analysis of axonal branches in GABAergic motor neurons in *B* and *C* was the same as in Figure 1A. (***) $P < 0.001$, Kruskal-Wallis test and Dunn's multiple comparison post-test.

and neuron-specific expression studies indicate that SSUP-72 functions cell-autonomously (Supplemental Fig. S4A,B), similar to CPSF-4 (Supplemental Fig. S1C) and PFS-2 (Van Epps et al. 2010).

The phosphatase activity of human Ssu72 is required for transcription-coupled polyadenylation in vitro when in a complex with symplekin (Xiang et al. 2010), whereas, in yeast, Ssu72 can affect 3′ end processing independently of its phosphatase activity (Krishnamurthy et al. 2004). To test whether the phosphatase activity of SSUP-72 is required for its function, we mutated the catalytic Cys13 or Asp145 to Ser or Ala, respectively (Fig. 2A). Expression of either mutant SSUP-72 (C13S or D145A) failed to rescue *ssup-72(0); sydn-1(0); syd-2(0)* and did not cause discernable defects in a wild-type background (Fig. 2B). Moreover, Western blot analysis using the 4H8 antibody, which was raised against Ser5P-CTD, showed increased CTD phosphorylation in *ssup-72(0)* and *sydn-1(0); ssup-72(0)* animals (Supplemental Fig. S4C–E).

The cyclin-dependent kinase Cdk7 can phosphorylate Ser5 of Pol II CTD (Phatnani and Greenleaf 2006). To further address whether regulated CTD Ser5 phosphorylation is involved in neuronal development, we examined *cdk-7(ax224ts)*, a partial loss-of-function mutation that displays decreased Ser2 and Ser5 phosphorylated CTD and maternal effect lethality at the restrictive temperature (Wallenfang and Seydoux 2002). *cdk-7(ax224ts)* mutants raised at the restrictive temperature showed grossly normal neuronal morphology (Supplemental Fig. S4G; data not shown) and strongly enhanced the axonal and behavioral defects of *sydn-1(0)* (Supplemental Fig. S4G), suggesting that reducing phosphorylated CTD impairs neuronal development in a manner sensitive to the function of *sydn-1*. Double mutants of *cdk-7(ax224ts); ssup-72(0)* showed no obvious neuronal defects (Supplemental Fig. S4G). Notably, the maternal effect lethality of *cdk-7(ax224ts)* at the restrictive temperature was partially suppressed by *ssup-72(0)* (Supplemental Fig. S4F). Taken together, these data provide further support for the conclusion that SSUP-72 phosphatase acts on the Ser5 phosphorylated CTD.

Since orthologs of the genes identified as *sydn-1(0)* suppressors are known to interact biochemically (Dichtl et al. 2002), we next addressed their functional dependency. Overexpression of *ssup-72(+)* or *cpsf-4(+)* rescued the suppression of *sydn-1(0)* by *ssup-72(0)* or *cpsf-4(lf)*, respectively, but did not rescue the suppression by *cids-1(0)* or *cids-2(0)* (Fig. 2C). Conversely, overexpression of *cids-2(+)* rescued the suppression of *sydn-1(0)* by *cids-2(0)* but not that by *ssup-72(0)* or *cpsf-4(lf)* (Fig. 2C). These data suggest that the proteins encoded by these *sydn-1(0)* suppressor genes act in a mutually dependent manner.

SYDN-1 can bind SSUP-72 and be coimmunoprecipitated with RNA Pol II

The genetic interaction between *sydn-1* and multiple NpolyA factors suggests that SYDN-1 inhibits the function of NpolyA factors. We next addressed how SYDN-1 might regulate SSUP-72. The overall levels of *ssup-72* mRNA were similar in *sydn-1(0)* and wild type (Supplemental Fig. S5B). Animals expressing a GFP::SSUP-72 translational fusion protein showed nuclear localization in multiple tissues, including the epidermis, intestine, and nervous system (Supplemental Fig. S5A); this pattern was not altered in *sydn-1(0)* mutants (Supplemental Fig. S5C). Similarly, *sydn-1(0)* did not alter the expression pattern of CPSF-4 (Supplemental Fig. S5D).

We next tested whether SYDN-1 might physically interact with SSUP-72. In the yeast two-hybrid assay, SYDN-1 interacted with SSUP-72, and this interaction involved the C-terminal half of SYDN-1 (amino acids 301–578) (Fig. 3A). As Ssu72 is known to bind the CTD of RNA Pol II

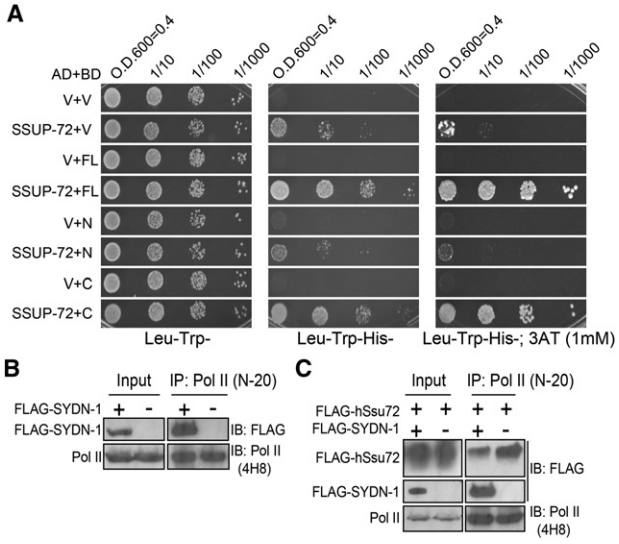

Figure 3. SYDN-1 can bind SSUP-72 and associate with RNA Pol II. (*A*) Interaction between SYDN-1 and SSUP-72 in a yeast two-hybrid assay. The SSUP-72 full-length protein fused to the GAL4 activation domain (AD) interacts with the SYDN-1 full-length protein or the CTD fused to the GAL4-binding domain (BD) and does not interact with the SYDN-1 N-terminal domain or GAL4-binding domain. Yeast cells were plated in a dilution series on selection plates of Trp^-Leu^- (*left*), $Trp^-Leu^-His^-$ (*middle*), and $Trp^-Leu^-His^-$ with 1 mM 3AT. (V) Empty vector; (FL) SYDN-1 full-length protein; (N) SYDN-1 (1–300 amino acids); (C) SYDN-1 (301–578 amino acids). (*B*) SYDN-1 can associate with human RNA Pol II. HEK293T cells were transfected with Flag-tagged SYDN-1, and cell lysates were immunoprecipitated with N-20 anti-Pol II antibodies recognizing the large subunit of RNA Pol II. Coimmunoprecipitated proteins were blotted with anti-Flag and 4H8 anti-Pol II CTD. Two percent of cell lysates were run as the input. (*C*) The presence of SYDN-1 can reduce the association of human Ssu72 with Pol II. HEK293T cells were transfected with the constructs indicated, and cell lysates were immunoprecipitated with N-20 anti-Pol II antibodies. Coimmunoprecipitated proteins were blotted with anti-Flag and 4H8 anti-Pol II CTD. One percent of immunoprecipitation lysates were run as the input.

(Xiang et al. 2010), we asked whether SYDN-1 could also associate with RNA Pol II. Because SYDN-1 expressed in *C. elegans* was highly insoluble (data not shown), we expressed Flag::SYDN-1 in HEK293T cells and found that it localized to subnuclear puncta (Supplemental Fig. S5E), consistent with its nuclear localization in *C. elegans* neurons (Van Epps et al. 2010). We then immunoprecipitated RNA Pol II using the N-20 antibody, which recognizes the large subunit of human RNA Pol II (Cheng and Sharp 2003), and consistently pulled down Flag::SYDN-1 (Fig. 3B). Human Ssu72 could also be coimmunoprecipitated with RNA Pol II (Fig. 3C). Interestingly, when we coexpressed SYDN-1 with human Ssu72, significantly less Ssu72 was coimmunoprecipitated with RNA Pol II (Fig. 3C). While it is possible that heterologous expression of SYDN-1 might lead to a dominant-negative effect of titrating human Ssu72, together with the genetic analysis and the observed protein interaction in yeast two-hybrid assay, these data suggest that SYDN-1 may interfere with the interaction between RNA Pol II and Ssu72.

Genome-wide analysis of RNA Pol II CTD occupancy identifies neuronal ankyrin UNC-44 as a target of SYDN-1 and SSUP-72

As the phosphorylation state of the RNA Pol II CTD is intimately linked to transcription (Buratowski 2009), we next examined CTD occupancy by performing chromatin immunoprecipitation (ChIP) using the 4H8 antibody followed by deep sequencing (ChIP-seq) (Supplemental Fig. S6A; Supplemental Material). We obtained comparable numbers of reads (~20 million for each) from ChIP-seq DNA libraries made from stage-matched worms of wild type; *sydn-1(0)* and *ssup-72(0)* single mutants; and *sydn-1(0); ssup-72(0)* double mutants (Supplemental Table S5). We mapped the unique reads to the *C. elegans* genome. About 4000 protein-coding genes exhibited Pol II occupancy with largely overlapping gene coverage among the four strains (Supplemental Figs. S6B, S7A,C).

The intergenic regions for many genes in *C. elegans* are generally short, with the transcription end site (TES) or transcriptional start site (TSS) of a gene often overlapping with neighboring genes. Through both manual inspection of the entire genome and bioinformatic analyses of well-annotated genes, we compared the CTD occupancy at nonoverlapping TESs (Supplemental Material). For most genes, the CTD occupancy pattern within ±500 base pairs (bp) flanking each TES was similar between wild type and *sydn-1(0)* (Supplemental Figs. S6C, S7B; Supplemental Excel Files S1–S3). Among the few genes with significant changes in CTD occupancy between *sydn-1(0)* and wild type, the ankyrin gene *unc-44* attracted our interest because it is known to undergo APA in neurons.

The *unc-44* locus spans >40 kb and generates multiple mRNA isoforms due to alternative TSSs, splicing, and polyadenylation (Fig. 4A; Boontrakulpoontawee and Otsuka 2002; Otsuka et al. 2002). *unc-44* mRNA isoforms encode several proteins containing the ankyrin domain in the N terminus. The last three exons encode a large protein domain unique to the neuronal ankyrin isoform UNC-44F. By careful inspection of Pol II CTD occupancy, we noticed a marked reduction of Pol II CTD binding at the last three exons of *unc-44* in *sydn-1(0)* compared with wild type, whereas Pol II CTD occupancy in the 5′ region of the gene was unchanged in *sydn-1(0)* (Fig. 4A; Supplemental Fig. S6C–E). *ssup-72(0)* showed normal Pol II CTD occupancy and suppressed the reduced Pol II CTD binding in *sydn-1(0)* (Supplemental Figs. S6C,D, S7B–D). We quantitated mRNA levels of *unc-44* using RT-qPCR. In *sydn-1(0)*, levels of *unc-44f* mRNA encoding the neuronal isoform were decreased to <10% of wild type, and this reduction was restored to above the wild-type levels in the *ssup-72(0); sydn-1(0)* double mutants (Fig. 4B). The levels of *unc-44* mRNA amplified using primers targeting a common region (*unc-44c*) were not significantly different among wild-type, *sydn-1(0)*, *ssup-72(0)*, and *sydn-1(0);*

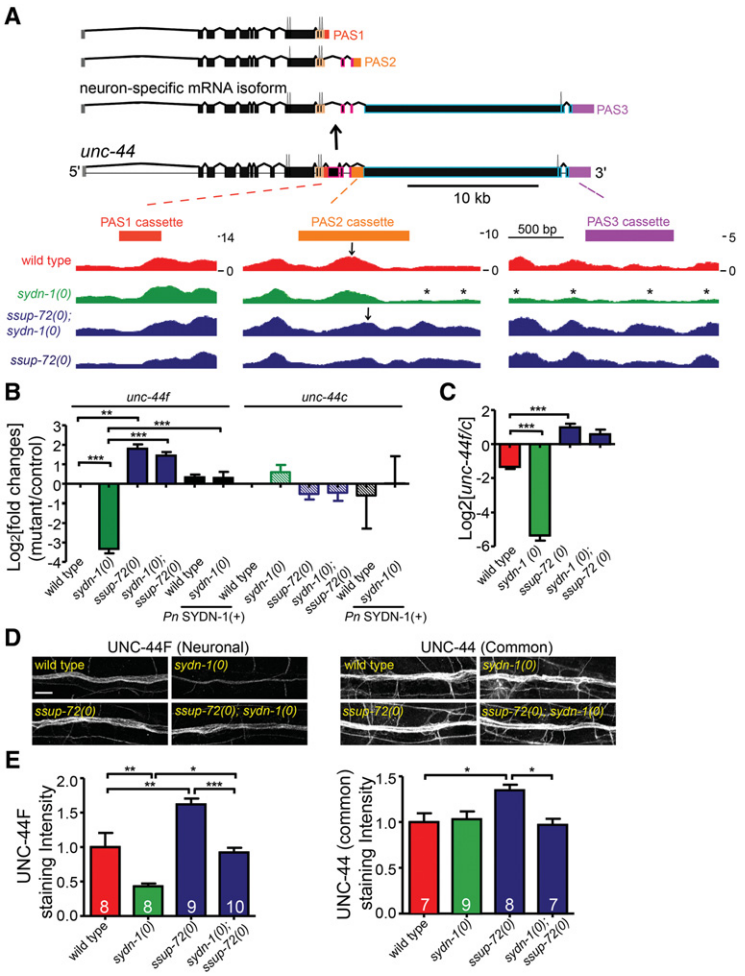

Figure 4. The expression of the neuron-specific *unc-44f* long isoform depends on SYDN-1 and SSUP-72. (*A*) 4H8 ChIP-seq analyses show a SYDN-1- and SSUP-72-dependent RNA Pol II CTD-binding pattern at the *unc-44* locus. *sydn-1(0)* shows a greater than twofold significant decrease in Pol II CTD binding in the coding region of the neuron-specific *unc-44f* isoform compared with wild type (Supplemental Material), which is reversed by *ssup-72(0)*. (*Top*) *unc-44* locus produces transcripts terminating at three PASs, and the usage of PAS3 is neuron-specific. Three PAS regions are enlarged *below*, and a few exons preceding the PAS cassette are outlined in colors. Black arrows indicate Pol II pausing at the *unc-44* PAS2 cassette. Asterisks indicate reduced Pol II binding after *unc-44* PAS2 in *sydn-1(0)*. (*B*) SYDN-1 and SSUP-72 interaction regulates the mRNA levels of *unc-44f*. cDNA libraries were constructed from mRNAs isolated from synchronized L2 worms. RT-qPCR analyses show that *unc-44f* in *sydn-1(0)* (solid bars) is reduced to <10% that of wild type; loss of function in *ssup-72* and pan-neuronal expression of *sydn-1* completely reversed this reduction. Total levels of *unc-44* common isoforms (slashed bars; *unc-44c*) show mild change. The histogram shows quantification of both *unc-44f* and *unc-44c* [for wild type and *sydn-1(0)*, $n = 9$; for *ssup-72(0)* and *ssup-72(0); sydn-1(0)*, $n = 6$; for *Pn-sydn-1* and *sydn-1(0); Pn-sydn-1*, $n = 3$]. *rps-25* was used as the internal control. Shown are the $\log_2$ values of fold changes between mutant strains and wild type. (**) $P < 0.01$; (***) $P < 0.001$, one-way ANOVA and Bonferroni's multiple comparison post-test. (*C*) *ssup-72(0)* further increases the mRNA levels of *unc-44f*. The ratio between *unc-44f* and *unc-44c* is decreased in *sydn-1(0)* and increased in *ssup-72(0)* and *ssup-72(0); sydn-1(0)* compared with wild type. Shown is the $\log_2$ value of the ratios between *unc-44f* and *unc-44c*. (***) $P < 0.001$, one-way ANOVA and Bonferroni's multiple comparison post-test. (*D*) Protein levels of the neuron-specific UNC-44F isoform is reduced in *sydn-1(0)*. Shown are confocal images of immunostaining of UNC-44 protein in the ventral cord in the genotypes indicated. Bar, 10 µm. (*E*) Quantification of UNC-44 immunostaining in the genotypes indicated. Confocal *Z*-stack images of the nerve cords (0.5-µm section, 15 sections per cord) were collected for quantitative analysis. Fluorescence intensities in different genotypes were normalized to the average intensity of wild type. Shown are normalized intensities ± SEM; *n* = number of animals. (*) $P < 0.05$; (**) $P < 0.01$; (***) $P < 0.001$, one-way ANOVA and Bonferroni's multiple comparison post-test.

ssup-72(0) animals (Fig. 4B). Moreover, pan-neuronal expression of *sydn-1(+)* fully rescued the reduction of *unc-44f* mRNA in *sydn-1(0)* (Fig. 4B). Thus, the production of the neuron-specific *unc-44f* mRNA isoform is dependent on neuronal expression of *sydn-1*.

To examine how the *sydn-1* pathway affected UNC-44 protein levels, we performed immunostaining using antibodies raised against the neuronal UNC-44F-specific domain or against the common region of all UNC-44 isoforms, which are expressed in many tissues (Otsuka et al. 2002). We quantitated UNC-44 staining intensity in the ventral nerve cord and found that UNC-44F-specific staining was decreased dramatically in *sydn-1(0)* compared with wild type and that this decrease was restored to wild-type levels in the *sydn-1(0); ssup-72(0)* double mutants (Fig. 4D,E, left panel images and left histogram). In agreement with the RT-qPCR results, the immunostaining intensity for common UNC-44 isoforms was unaffected in *sydn-1(0)* single mutants (Fig. 4D,E, right panel images and right histogram). Together, these analyses show that SYDN-1 is specifically required for expression of the neuronal ankyrin UNC-44F isoform via its interaction with SSUP-72.

Loss of ssup-72 *function prevents transcription termination at a strong PAS in the coding region of* unc-44

By 3′RACE analyses, we validated two major PASs within the coding region of *unc-44*, for simplicity named PAS1, PAS2 (present in mRNAs expressed in many tissues), and PAS3 (present only in the neuronal *unc-44f* mRNAs) (Otsuka et al. 2002; Supplemental Fig. S8A,B). All three PASs are composed of the canonical PAS AAUAAA (Supplemental Table S4). We analyzed 3′RACE products and found that *sydn-1(0)* or *ssup-72(0)* alone did not alter the use of poly(A) addition sites of *unc-44* transcripts (Supplemental Fig. S8A,B). In *sydn-1(0)* animals, the amount

of PAS3 usage was noticeably reduced, while those of PAS1 and PAS2 showed no detectable changes from wild type (Supplemental Fig S8A–C). Interestingly, by RT-qPCR analyses, we found that, in *ssup-72(0)* and *sydn-1(0); ssup-72(0)*, the ratio between the *unc-44f* and *unc-44c* isoforms was higher than that in wild type (Fig. 4C, right panel). Moreover, Pol II CTD pausing at the endogenous PAS2 region of *unc-44* was noticeably shifted in *ssup-72(0)* animals (Figs. 4A, 5A; Supplemental Fig. S9A, B), suggesting that production of *unc-44f* may be dependent on the regulation of internal PASs.

To specifically examine how *sydn-1* and *ssup-72* regulate 3′ end processing of *unc-44* mRNA in neurons, we next generated a set of mini-expression constructs driven by a pan-neuronal promoter (Supplemental Table S2). In these constructs, the sequences of *unc-44* PAS1 or PAS2 cassettes, including the corresponding terminal introns, were placed downstream from the GFP coding sequence (Fig. 5B,C). To mimic the competition between internal and distal PASs, we placed the 3′ end sequences of the muscle myosin *unc-54* gene downstream from the *unc-44* internal PAS1 or PAS2 cassettes, respectively (Fig. 5B,C). CTD occupancy at the endogenous *unc-54* PAS locus was not dependent on SYDN-1 or SSUP-72 (data not shown). To precisely compare transcription-coupled 3′ end processing from these reporters in vivo, we generated single-copy integrated transgenes (Mos-SCI) at the same locus (Supplemental Table S2).

We verified by 3′RACE analysis that, in wild-type animals, the usage of PAS1 and PAS2 in the minireporters recapitulated that at the endogenous *unc-44* locus (Fig. 5B, C). We did not detect usage of the downstream *unc-54* 3′ PAS in either reporter, indicating that these two internal PASs are strong signals for 3′ end processing and transcription termination. *sydn-1(0)* did not alter the usage of either PAS1 or PAS2 in these reporters (Fig. 5B,C). However, in *ssup-72(0)* or *ssup-72(0); sydn-1(0)* mutants, we observed increased usage of the downstream *unc-54* PAS from the PAS2 reporter (Fig. 5C). The PAS1 reporter showed no changes in *ssup-72(0)* or *ssup-72; sydn-1(0)* (Fig. 5B). These data suggest that loss of *ssup-72* function caused compromised transcription termination at PAS2. Based on the observation that transcription from the PAS2 reporter proceeds to the distal *unc-54* PAS when *ssup-72* is absent, we infer that inhibition of SSUP-72 phosphatase activity by SYDN-1 at the PAS2 region of the endogenous *unc-44* locus is required for producing the neuron-specific *unc-44f* isoform.

Dysregulation of unc-44f *transcripts contributes to the neuronal phenotypes of* sydn-1 *mutants*

To examine whether dysregulated APA of *unc-44* might contribute to the neuronal defects in *sydn-1(0)*, we next performed genetic interaction studies. The long isoform of *unc-44* is required for axonogenesis

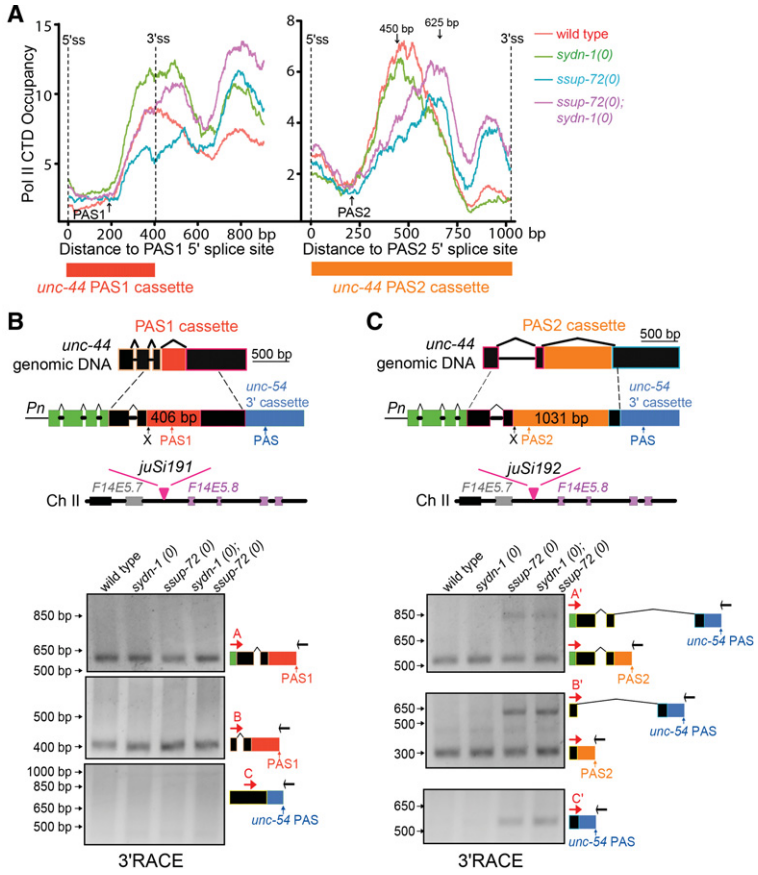

Figure 5. SSUP-72 regulates 3′ end processing at the strong internal PAS2 of *unc-44*. (*A*) Shown are RNA Pol II CTD occupancy around the PAS1 (red bar *below* the *left* graph) and PAS2 (orange bar *below* the *right* graph) cassettes of *unc-44* in wild type and mutants as indicated. 5′ss and 3′ss and the dashed lines denote the 5′ and 3′ splice sites flanking each cassette. Peak location of RNA Pol II CTD occupancy in the PAS2 cassette is around the 450-bp position (5′ splice site being 0) in wild type and *sydn-1(0)* and is shifted to 625 bp in *ssup-72(0)* and *ssup-72(0); sydn-1(0)*. (*B*) *sydn-1* and *ssup-72* do not affect the usage of the internal PAS1 of *unc-44*. (*Top* panel) Schematic illustration of the GFP reporter for the *unc-44* PAS1 cassette (*juSi191*) inserted on chromosome II. (*Bottom* panel) Images of DNA electrophoresis gels of 3′RACE results of the PAS1 reporter using three different gene-specific primers (red arrows) and reverse adaptor primer (black arrows) in the genotypes indicated; the illustrations represent the sequences of the PCR fragments. No products were amplified for primer C. (*C*) Loss of function in *ssup-72* results in pre-mRNA 3′ end processing at the distal *unc-54* PAS in addition to the internal PAS2 of *unc-44*. (*Top* panel) Schematic illustration of the GFP reporter for the *unc-44* PAS2 cassette (*juSi192*) inserted on chromosome II. (*Bottom* panel) Images of DNA electrophoresis gels of 3′RACE results of the PAS2 reporter using three different gene-specific primers (red arrows) and reverse adaptor primer (black arrows) in the genotypes indicated; illustrations represent the sequences of the PCR fragments. (X) Stop codon.

(Boontrakulpoontawee and Otsuka 2002). *unc-44* (*tm349*) is a deletion within the large *unc-44f*-specific exon, and homozygous mutants are severely uncoordinated and slow-growing. The axonal defects in *unc-44 (tm349)* animals resembled those in *unc-44(e362*), a mutation affecting all isoforms (Boontrakulpoontawee and Otsuka 2002). To test whether reducing neuronal UNC-44F contributes to the *sydn-1(0)* phenotype, we constructed *sydn-1(0); unc-44(tm349)/nT1* (*nT1* is a chromosomal balancer for propagation). By RT-qPCR analysis, we observed significant reduction of *unc-44f* in the *unc-44 (tm349)/nT1* animals compared with controls (Fig. 6A). Based on the RT-qPCR analysis (Fig. 4B), we estimated that, in *sydn-1(0)*, the *unc-44f* mRNA levels were <10% of wild-type levels. We predicted that any further decrease of *unc-44f* in the *unc-44(tm349)/nT1* heterozygotes should induce a more severe phenotype (Fig. 6A). Indeed, heterozygosity for *unc-44(tm349)* significantly enhanced the axon branching phenotype in *sydn-1(0)* but had no effect in a *sydn-1(+)* background (Fig. 6B). As a control for the specificity of *unc-44f* dosage-dependent enhancement of axon defects on *sydn-1(0)*, we tested *syd-2(0)* mutants and observed no discernable difference in axon morphology among animals containing *nT1*/+ or *unc-44(tm349)/nT1* (Fig. 6B). The sensitivity of *sydn-1(0)* to reduced *unc-44* gene dosage is consistent with the *sydn-1(0)* mutant displaying lower UNC-44F expression.

We also addressed whether removing PAS2 of *unc-44* could increase the expression of *unc-44f* mRNA, thereby suppressing *sydn-1(0)*. Using CRISPR genome-editing technology, we generated two mutations, *ju1377* and *ju1378*, which removed 83 bp and 180 bp containing the polyadenylation consensus sequence in the PAS2 cassette, respectively (Fig. 6C; see the Materials and Methods). Both alleles showed increased production of *unc-44f* by 3′RACE (Fig. 6C) and suppressed the movement defects of *sydn-1 (0); syd-2(0)* double mutants (Materials and Methods). Single mutants of either allele showed normal neuronal morphology and strongly suppressed the axon morphology defects of *sydn-1(0)* (Fig. 6D). Thus, we conclude that pre-mRNA processing of *unc-44f* in neuronal development depends critically on the regulation of internal PAS2 by the SYDN-1 and SSUP-72 pathway.

Usage of a weak coding region PAS of dlk-1 *also depends on SYDN-1 and SSUP-72*

To explore whether the SYDN-1 pathway might have a broader role in regulating APA, we tested several other neuronal genes that produce multiple mRNA isoforms by APA

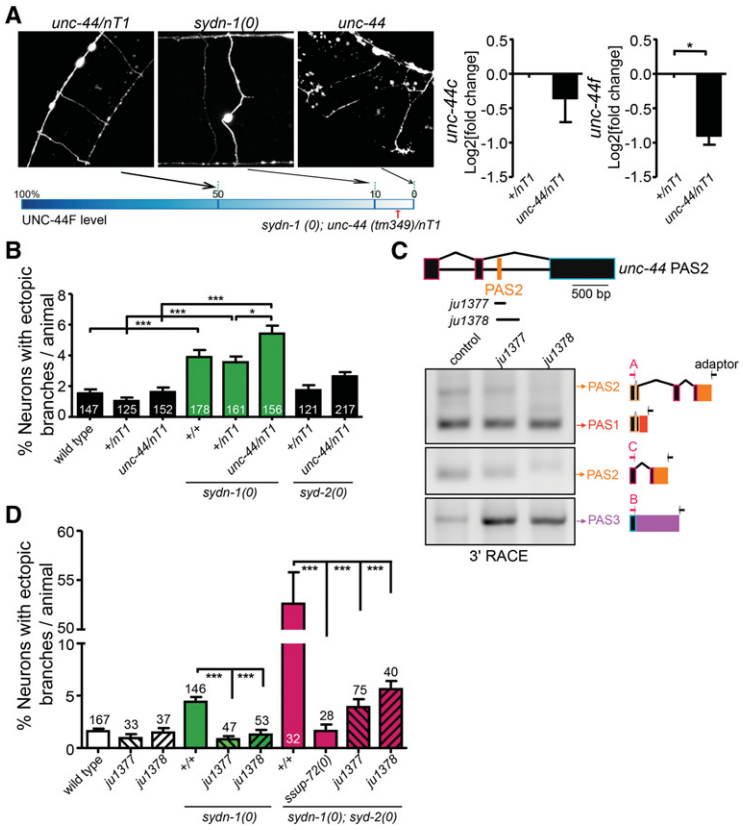

Figure 6. Dysregulated APA of *unc-44* causes neuronal defects of *sydn-1* mutants. (*A*) Levels of *unc-44f* mRNA correlate with axonal morphology defects. Shown at the *left* are images of axonal morphology of the GABAergic motor neurons labeled by *juIs76 [Punc-25-GFP]* in the genotypes indicated. *Below* is a diagram depicting the functional correlation to the levels of UNC-44F in *sydn-1* and *unc-44*. The two graphs at the *right* show the mRNA levels of *unc-44c* and neuron-specific *unc-44f* ($n = 3$). Shown is the $\log_2$ value of fold changes between +/*nT1* and *tm349/nT1* strains. (*) $P < 0.05$, paired *t*-test. *rps-25* was used as the internal control. (*B*) Reduced *unc-44f* dosage in *sydn-1(0)* mutants induces more severe defects in neurons. The graph shows quantification of the average percentage of abnormal neurons with ectopic axonal branches per animal. Data are shown as mean ± SEM; n = number of animals. (*) $P < 0.05$; (***) $P < 0.001$, Kruskal-Wallis test and Dunn's multiple comparison post-test. (*C*) Deletion mutations of the PAS2 at the endogenous *unc-44* locus cause increased polyadenylation at PAS3 of *unc-44* compared with *sydn-1(0)*. The *top* illustration shows the location of *ju1377* and *ju1378* mutations around PAS2 (also see Supplemental Table S4). Images show 3′RACE analyses of *unc-44* transcripts in *sydn-1(0); syd-2(0)* (*left* lane), *unc-44(ju1377); sydn-1(0); syd-2* (*middle* lane), and *unc-44(ju1378); sydn-1(0); syd-2(0)* (*right* lane). Black arrows are the reverse adaptor primer commonly used in the 3′RACE kit; gene-specific primer A amplifies both PAS1 and PAS2, gene-specific primer B amplifies PAS3, and gene-specific primer C amplifies PAS2. Sequences of the amplified DNA fragments corresponding to each band are shown as an illustration. (*D*) Ectopic branches of GABAergic motor neurons in *sydn-1(0)* are suppressed by deletion mutations of *unc-44* PAS2. Shown is the quantification of the average percentage of GABAergic neurons that display ectopic branches in the genotypes indicated. Fifteen to 19 commissures per adult animal were counted. (***) $P < 0.001$, Kruskal-Wallis test and Dunn's multiple comparison post-test. Bar, 10 µm.

and identified a distinct mode of regulation in the *dlk-1* gene, which encodes a conserved MAPKKK (Nakata et al. 2005). *dlk-1* produces two protein isoforms, DLK-1L (long) and DLK-1S (short) (Yan and Jin 2012), with *dlk-1S* transcripts generated using an intronic PAS (Fig. 7A). While the PAS usage of *dlk-1L* showed no difference between wild type and *sydn-1(0)*, *dlk-1S* PAS usage was virtually undetectable in *sydn-1(0)* (Supplemental Fig. S3). Moreover, transgenic reporters containing GFP::DLK-1S coding sequences followed by the *dlk-1S* 3′ end cassette showed consistently decreased GFP levels in *sydn-1(0)* compared with wild type, and *ssup-72(0)* suppressed this reduction in GFP expression (Supplemental Fig. S10A, left panel and histogram, *juEx5216*). Neither *sydn-1(0)* nor *ssup-72(0)* affected expression of a control transgene with the *unc-54* PAS cassette (Supplemental Fig. S10A, right panel and histogram, *juEx5272*). These results suggest that SYDN-1 promotes the expression of *dlk-1S*.

To further test how the usage of the *dlk-1S* PAS was affected in *sydn-1(0)* and *ssup-72(0)*, we generated an integrated single-copy *dlk-1S* PAS reporter transgene containing the *dlk-1S* 3′ end cassette flanked by exon 7 and exon 8 sequences and followed by the *unc-54* PAS cassette (Supplemental Fig. S10B, *juSi186*, left panel). 3′RACE analysis of this *dlk-1S* PAS reporter identified one major product that corresponded to the spliced transcripts ending with the *unc-54* PAS (Supplemental Fig. S10B, right panel). This observation indicates that the *dlk-1S* PAS is a weak signal for 3′ end processing and may be outcompeted by the splicing of *dlk-1* intron 7.

To sensitize the detection of the *dlk-1S* PAS, we mutated the splice sites of intron 7 (Fig. 7A, *juSi243*, left panel). By 3′RACE analyses, we obtained multiple products generated from the *juSi243* line, and analyses of their sequences showed that these transcripts terminated at either the *dlk-1S* PAS or the PAS of a neighboring gene, *F14E5.8*, located 3′ to the integration site (Fig. 7A). In wild type, 19% of the DNA clones ($n = 22$) showed usage of the *dlk-1S* PAS, comparable with *sydn-1(0)* (14% colonies, $n = 22$) (Fig. 6C, right panel). Interestingly, *ssup-72(0)* greatly increased the usage of the *dlk-1S* PAS in *juSi243*, as, in *ssup-72(0)* single and *ssup-72(0); sydn-1(0)* double mutants, *dlk-1S* PAS usage was increased to 40% ($n = 23$) and 60% ($n = 20$), respectively (Fig. 7A, right panel). These data are consistent with the model that SYDN-1 promotes the usage of the weak *dlk-1S* PAS by inhibiting SSUP-72 function.

DLK-1S binds and inhibits DLK-1L (Yan and Jin 2012). Decreasing levels of DLK-1S elevate the activity of DLK-1L. To address whether up-regulation of DLK-1L activity contributed to the *sydn-1(0)* phenotype, we generated double mutants of *sydn-1(0); dlk-1(0)*. *dlk-1(0)* suppressed the ectopic axonal branches of *sydn-1(0)* single and *sydn-1(0); syd-2(0)* double mutants (Fig. 7B). These data support a conclusion that the aberrant axon morphology of the *sydn-1(0)* mutant likely results from dysregulation of APA in multiple neuronal genes and underscore the complexity of context-dependent APA.

Discussion

APA empowers regulation of gene expression and cellular activities at multiple levels. Although much has been learned about the biochemical reactions mediating cleavage and polyadenylation of pre-mRNAs, how alternative 3′ ends of pre-mRNAs are selected in vivo remains poorly understood. Here, guided by the genetic interactions

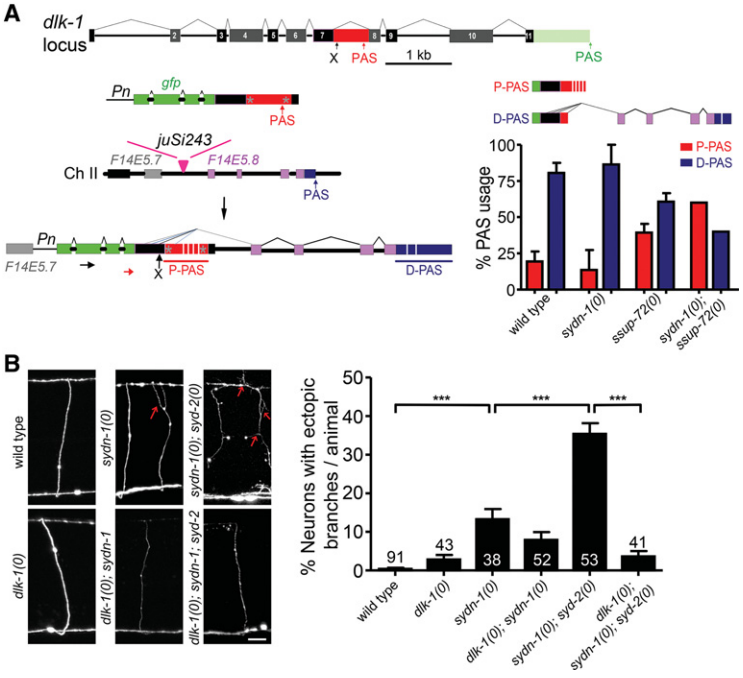

Figure 7. Dysregulated APA of *dlk-1* contributes to neuronal defects of *sydn-1* mutants. (*A*) Loss of function in *ssup-72* can promote the usage of the internal *dlk-1S* PAS. (*Left* panel) Illustration of the GFP reporter for the *dlk-1S* PAS (*juSi243*) inserted on chromosome II. The *F14E5.8* gene follows the insertion site. Splice sites of the PAS-containing intron are mutated (gray asterisks). Cryptic splice sites and PASs are labeled. Primers for 3′RACE are shown. (*Right* panel) Quantification of sequencing results from 3′RACE products of the *juSi243* reporter in the genotypes indicated. 3′RACE products were cloned into pCR8. For each genotype, >20 colonies were sequenced (for wild type, $n = 22$; for *sydn-1(0)*, $n = 22$; for *ssup-72(0)*, $n = 23$; for *ssup-72(0); sydn-1(0)*, $n = 20$). (X) Stop codon. (*B*) Ectopic branches of GABAergic motor neurons in *sydn-1(0)* are suppressed by *dlk-1(0)*. Shown at the *left* are images of axon morphology of the GABAergic motor neurons labeled by *juIs76 [Punc-25-GFP]* in the genotypes indicated. Red arrows indicate abnormal branches. The graph at the *right* shows the quantification of the average percentage of GABAergic neurons that display ectopic branches in the genotypes indicated. Five to six commissures per L1 animal were counted. (***) $P < 0.001$, Kruskal-Wallis test and Dunn's multiple comparison post-test. Bar, 10 µm.

between *sydn-1* and *ssup-72* or select NpolyA factors, we uncovered a molecular mechanism regulating coding region APA of two genes important for the development of the nervous system. We propose that the interaction between SYDN-1 and SSUP-72 at internal PASs regulates APA in a context-dependent manner (Supplemental Fig. S11).

SSUP-72 controls APA within coding regions

Ankyrins provide scaffolds for cells and act as adaptors for signaling pathways (Cunha and Mohler 2009). In *C. elegans*, the *unc-44* locus generates multiple isoforms of ankyrin, using APA to meet the needs of different cell types (Otsuka et al. 2002). Transcripts encoding the neuron-specific UNC-44F isoform are reduced in *sydn-1(0)* mutants, and this reduction is restored to wild-type levels by loss of function in *ssup-72* or select NpolyA factors (Fig. 4; data not shown). Using PAS reporters that create a competitive APA configuration between the coding region PAS of *unc-44* and the PAS of *unc-54* at the distal location, we show that *unc-44* coding region PAS1 and PAS2 are strong PASs for 3′ end processing. In *ssup-72(0)* mutants, the use of the coding region *unc-44* PAS2 is weakened, enabling transcription to proceed and terminate at a distal PAS regardless of the distance or sequence nature of the distal PAS. In *sydn-1(0)* mutants, transcription terminates at PAS2 of the endogenous *unc-44* locus, and the production of the *unc-44f* mRNA is reduced. The observed function of SSUP-72 is highly specific to PAS2, as the usage of *unc-44* PAS1, which also is a strong PAS for 3′ end processing, is unaffected by *ssup-72(0)*. Furthermore, compared with wild type, the ratio of *unc-44f* mRNA to *unc-44c* mRNA is lower in *sydn-1(0)* and higher in *ssup-72(0)* or *ssup-72(0); sydn-1(0)*, suggesting that SYDN-1 may function to balance SSUP-72 activity at the coding region PAS2 of *unc-44* to promote 3′ end processing of distal PASs. Importantly, we show that polyadenylation of *unc-44f* mRNA is restored in genetic mutants in which usage of PAS2 is compromised, resulting in behavioral and neuronal morphology suppression of *sydn-1(0)* animals.

The negative regulation of SSUP-72 by SYDN-1 can also promote the expression of the *dlk-1S* isoform. The *dlk-1S* PAS contains a noncanonical polyadenylation hexamer. In our reporter assay, the *dlk-1S* PAS behaves as a weak signal for 3′ end processing, and loss of function in *ssup-72* facilitates the use of the *dlk-1S* PAS. The usage of the weak *dlk-1S* PAS appears to depend on the splicing of the intron containing the *dlk-1S* PAS, suggesting that splicing and 3′ end processing are coordinated at this PAS. Our genetic studies demonstrate that dysregulation of APA in *dlk-1* results in functional defects, consistent with its roles in neuronal development. Future studies will tease apart the molecular underpinning for such context-dependent regulation of APA.

Regulation of RNA Pol II CTD phosphorylation is coupled with coding region APA

The phosphorylation and dephosphorylation cycle on RNA Pol II CTD has been proposed to provide codes for transcription-coupled pre-mRNA processing (Egloff and Murphy 2008; Buratowski 2009). The interplay between CTD kinases and phosphatases therefore strongly affects the status of mRNA transcription at multiple steps, as differentially phosphorylated CTD can recruit interacting proteins and affect the dynamics of transcription-coupled events. For example, Thr4 phosphorylation of the CTD by CDK9 is required for histone mRNA 3′ end processing (Hsin et al. 2011). Ser2 phosphorylation of the CTD is required for its association with polyadenylation factors (such as Pcf11) and for 3′ end processing of pre-mRNAs in yeast (Licatalosi et al. 2002; Ahn et al. 2004; Meinhart and Cramer 2004). The ratio of Ser5 phosphorylated CTD to Ser2 phosphorylated CTD is high at 5′ ends and low at 3′ ends (Komarnitsky et al. 2000). Ser7 phosphorylation of the CTD coincides with introns in budding yeast (Kim et al. 2010a). Ssu72 has a high degree of specificity for CTD Ser5 (Krishnamurthy et al. 2004; Xiang et al. 2010), although low activity on Ser7 has also been observed (Bataille et al. 2012; Xiang et al. 2012; Zhang et al. 2012). In human embryonic stem cells, Ssu72 is detected at introns by ChIP-seq (Chen et al. 2014). We speculate that dephosphorylation on Ser5P or Ser7P of the CTD at internal PASs by SSUP-72 helps to recruit select NpolyA factors and regulate 3′ end processing at internal PASs.

In other organisms, the phosphatase activity of Ssu72 is regulated by its binding partners. In yeast, Ssu72 binds Pta1 (He et al. 2003), whereas, in mammals, Ssu72 binds symplekin. Symplekin and Pta1 share weak sequence similarity, but both can facilitate Ssu72 phosphatase activity (Krishnamurthy et al. 2004; Xiang et al. 2010). We found that loss of function in *symk-1* also suppresses *sydn-1(0)*, consistent with *C. elegans* SYMK-1 being a functional partner of SSUP-72. Our protein interaction studies show that the presence of SYDN-1 reduces Pol II-associated Ssu72. Therefore, SYDN-1 may regulate SSUP-72 phosphatase activity by interfering with its interaction with Pol II.

In yeast, Ssu72 is essential for viability (Sun and Hampsey 1996), presumably because of its multiple functions in transcription (Dichtl et al. 2002; Steinmetz and Brow 2003; Krishnamurthy et al. 2004; Reyes-Reyes and Hampsey 2007). In contrast, we found that *C. elegans* SSUP-72 is dispensable for viability, fertility, and general development of the animals and instead plays a highly specific regulatory role in coding region APA. The growth defects of yeast *ssu72* cells are suppressed by *rpb2* and 6-azauracil, a drug impairing the enzyme required for synthesis of UTP and GTP, leading to the hypothesis that Ssu72 may normally attenuate the elongation rate of RNA Pol II (Dichtl et al. 2002). Although we did not observe an overall alteration of the CTD-binding pattern in *ssup-72(0)* mutants, high-resolution analysis of RNA Pol II CTD occupancy at the *unc-44* PAS2 cassette revealed a noticeable peak shift in *ssup-72(0)* mutants (Fig. 5A). It is possible that SSUP-72 affects transcription elongation rates at internal PASs. Additionally, chromatin microenvironments at internal PASs of *unc-44* or *dlk-1* may contribute to increased pausing of RNA Pol II or successful splicing to allow differential regulation of internal PASs.

Regulatory role of NpolyA factors in neuronal APA

The other NpolyA factors identified as genetic suppressors of *sydn-1(0)* either are in the CPSF complex, which functions in PAS recognition, or are CTD-binding proteins (Van Epps et al. 2010; and this study). While null mutants for these NpolyA genes are lethal and sterile, the development of the nervous system is remarkably normal. Conceivably, maternal contribution may provide sufficient activity for these proteins in neuronal differentiation and maintenance; we favor an alternative interpretation that select core NpolyA factors have substantial redundancy, and therefore elimination of individual factors is not detrimental for pre-mRNA processing in neurons. Null mutations in these NpolyA genes suppress *sydn-1(0)* to the same extent as *ssup-72(0)*. Moreover, overexpression of an individual factor cannot bypass the requirement of the other. Thus, these proteins also function in a mutually dependent manner to coordinate APA, acting to terminate the transcription at the strong internal *unc-44* PAS2 or promoting splicing at the weak internal *dlk-1S* PAS. Consistent with this idea, recent studies of mammalian CPSFs have linked their function to RNA Pol II pausing (Nag et al. 2007) and splicing (Martinson 2011; Misra et al. 2015).

Studies in human cells have identified >85 proteins as components of the 3′ processing complex, among which 50 additional proteins may mediate coupling with other cellular processes (Shi et al. 2009). Genetically, SYDN-1 interacts with NpolyA machinery but is specifically required for neuronal development. Importantly, from global assessment of polyadenylation events and genome-wide CTD occupancy assays, we did not detect major defects in PAS recognition in *sydn-1(0)*, indicating that SYDN-1 does not alter the basal function of transcription and 3′ end processing. Instead, SYDN-1 controls APA in neurons by modifying the phosphorylation state of the RNA Pol II CTD at intronic PASs. Overall, our findings reveal a previously unknown mechanism controlling coding region APA for transcript diversification in the nervous system.

Materials and methods

C. elegans *genetics*

Strains were maintained on NGM plates at 20°C–22.5°C as described (Brenner 1974). Genetic mutations used in this study are summarized in Supplemental Table S1. Double and triple mutants were constructed following standard procedures, and the genotypes were confirmed by DNA sequencing or restriction enzyme digestion of PCR fragments amplified using primers listed in Supplemental Table S1. Supplemental Table S2 lists all of the transgenes and strains used.

Transgenes of extrachromosomal arrays were generated following standard procedures (Mello et al. 1991). Expression constructs were injected at 1–20 ng/µL with coinjection marker *Pttx-3-RFP* at 50 ng/µL and pBlueScript to bring the total plasmid concentration to 100 ng/µL. For each construct, two to three independent transgenic lines were analyzed (Supplemental Table S2). MosSCI lines were generated at the chromosome II ttTi5605 site using EG6699 as described (Frokjaer-Jensen et al. 2008). Single-copy insertions were verified by LongAmp amplification using primers designed by M. Nonet (http://thalamus.wustl.edu/nonetlab/resourcesf/resources.html).

Fluorescence microscopy for synapse and axon morphology

Synaptic puncta were scored under the Zeiss Axioskop from the entire dorsal cord of strains containing *juIs1 [Punc-25-SNB-1::GFP].* Axonal branches of GABAergic motor neurons visualized by *juIs76 [Punc-25-GFP]* were counted from five to six commissures of L1 worms or 15–19 commissures of adult worms. Percentages of neurons with ectopic branches per animal were counted by dividing commissure number with abnormal branches by total commissure number scored from each worm. For quantitative confocal imaging, 1-d-old adult worms were paralyzed in M9 buffer containing 0.5%–1% 1-phenoxy-2-propanol (TCL America). A Zeiss LSM510 or LSM710 confocal microscope equipped with Chroma HQ filters was used for collecting images. To compare the intensity of immunostaining or GFP reporter genes from different strains, we imaged the dorsal or ventral nerve cord around the vulval region. Images were processed using MetaMorph software with genotypes blinded to the observer. Average fluorescence intensity in axons was measured after drawing a line along the dorsal nerve cord and subtracting the background from the nearby area; average nuclear fluorescence intensity was measured after outlining individual nuclei and subtracting the background. The average fluorescence intensity of mutants was normalized to that of wild type.

RT–PCR and 3′RACE analyses of mRNA

Total RNA was isolated using TRIzol (Invitrogen) from synchronized L1 or L2 worms cultured under the same conditions. Total RNA (2–5 µg) was reverse-transcribed into 20 µL of cDNA library using an oligo dT primer (Invitrogen, 18080-051) or an adaptor primer containing oligo dT sequences (Invitrogen, 18373-019). For semiquantitative PCR amplification, 1/20 vol of cDNA library, amplified using oligo dT primer, was used. RT-qPCR was conducted using the iQ SYBR Green Supermix kit (Bio-Rad) on a CFX96TM real-time system (C1000TM ThermalCycler, Bio-Rad). For each RT-qPCR reaction, 1/60 vol of cDNA library, amplified using oligo dT primer, was mixed with iQTM SYBR Green Supermix. Triplicate reactions were performed for each primer pair. The internal control *rps-25* was done in parallel with other primer pairs. Data were analyzed using CFX manager software (version 2, Bio-Rad). Primers for detecting transcripts of *ssup-72*, *ama-1*, *unc-44*, *gfp*, and *rps-25* in RT–PCR or RT-qPCR are listed in Supplemental Table S3. In 3′RACE, gene-specific or nested primers listed in Supplemental Table S3 were used together with adaptor primers for the first or second round of PCR amplifications of 3′ ends of *unc-44*, *dlk-1*, and *gfp* reporters. In the first amplification, 1/20 vol of cDNA library, amplified using adaptor primer, was used, and 2 µL of the first PCR product was used in the second amplification.

Statistical analysis

Statistical significance between two samples was determined in Prism (GraphPad Software) by the two-tailed Student's *t*-test if the samples followed Gaussian distribution or the Mann-Whitney test if they did not. To compare multiple samples, the statistical significance between any two samples was determined by one-way ANOVA if all samples followed Gaussian distribution; otherwise, Kruskal-Wallis test was used. To determine how two specific samples differed in multiple samples, a post-hoc test of Bonferroni's or Dunn's multiple comparison was conducted after

one-way ANOVA or Kruskal-Wallis test. For quantification of Western blot and RT-qPCR, paired *t*-test or one-way ANOVA was used.

3′ UTRome profiling and Pol II occupancy assay

3′ UTR libraries were constructed and sequenced as described (Mangone et al. 2010). ChIP-seq was performed as described (Mukhopadhyay et al. 2008). Additional details and data analyses are in the Supplemental Material.

Cell culture, transfection, and coimmunoprecipitation

HEK293T cells were cultured in Dulbecco's modified Eagle's medium (DMEM). Full-length *sydn-1* and human *ssu72* cDNAs were cloned into pcDNA3-Flag to generate tagged proteins. Cells were transfected by X-tremeGENE 9 DNA transfection reagent (Roche). Three days after transfection, cell lysates were prepared in RIPA buffer (25 mM Tris-HCl at pH 7.4, 150 mM KCl, 5 mM EDTA, 1% NP-40, 1% sodium deoxycholate, 0.1% SDS) with protease inhibitor cocktail (Roche) and phosphatase inhibitor cocktails (Sigma, P0044 and P5726). Equivalent amounts of lysates were incubated with anti-Pol II-bound (N-20, Santa Cruz Biotechnology, sc-899X) Dynabeads Protein A/G (Novex by Life Technologies) overnight at 4°C. After four washes, the bound proteins were eluted by heating for 5 min at 95°C in 2× Laemmli sample buffer (Bio-Rad) and resolved by SDS-PAGE. The coimmunoprecipitated proteins were blotted with primary mouse anti-Flag (Sigma, F3165), rabbit anti-Pol II (N-20; Santa Cruz Biotechnology, sc-899X), or mouse anti-Pol II (CTD4H8; Santa Cruz Biotechnology, sc-47701) antibody and visualized with HRP-conjugated anti-mouse or anti-rabbit secondary antibody (Amersham) at 1:5000 dilution using SuperSignal West Pico kit (Thermo Scientific).

Yeast two-hybrid assay

Bait and prey were cloned into pACT2 containing the GAL4 activation domain and pBTM166 containing the GAL4 DNA-binding domain (Clontech). Plasmids encoding activation domain fused SSUP-72 (pCZGY2665) or activation domain-only control were cotransformed with plasmids encoding the binding domain fused full-length SYDN-1 (pCZGY2666), the N-terminal half of SYDN-1 (pCZGY2667), or the C-terminal half of SYDN-1 (pCZGY2668) or the binding domain only into the L40 yeast strain and selected on $Trp^{-}Leu^{-}$ plates to obtain cotransformants. Single colonies were picked from each plate and cultured until $OD_{600} = 0.4–1.0$. Yeast cells were pelleted by centrifugation, washed twice with ddH_2O, and resuspended in ddH_2O. Five microliters of yeast cells per spot was plated on Histidine selection plates with or without 1 mM 3AT in a dilution series.

Generation of unc-44(ju1377) *and* unc-44(ju1378) *by CRISPR/Cas9-mediated genome editing*

We designed two sgRNAs around the polyadenylation consensus sequence (marked red in Supplemental Table S4) in the PAS2 cassette of *unc-44* (ATTAACCGACATATACGAAT and GTTCCA ATTGCTCCTGCCAT). We generated sgRNA plasmids using the P*eft-3-cas9*-NLS-pU6-sgRNA vector (pDD162; Addgene, #47549) by PCR-based site-directed mutagenesis as described (Dickinson et al. 2013). A mixture of P*eft-3-cas9*-NLS-pU6-sgRNA plasmids (100 ng/µL each pCZGY2855 and pCZGY2856) and 5 ng/µL P*myo-3*-mCherry (as a coinjection marker) was injected into 30 P0 1-d-old adults of *sydn-1(0); syd-2(0); juIs76*. We obtained 16 F1s with mCherry expression. From the progeny of two F1s, we observed worms showing improved locomotion and isolated them as *ju1377* and *ju1378*. We determined by DNA sequence analysis that *ju1377* and *ju1378* contained 83-bp and 180-bp deletions in the PAS2 cassette, respectively (highlighted in Supplemental Table S4).

Acknowledgments

We thank Rui Xiao for providing primers and protocols of RNA Pol II CTD ChIP-seq, Anthony Otsuka and Lihsia Chen for providing antibodies for UNC-44, Ya Dai for her contribution to the isolation of several *sydn-1(0)* suppressors, Dong Yan for discussion on *dlk-1S*, and Shohei Mitani (the Japanese National Bioresource Project) and the *C. elegans* gene knockout consortium for deletion alleles. We thank members of the Jin and Chisholm laboratories for help and comments. Some strains were obtained from the *Caenorhabditis* Genetics Center, which is supported by National Institutes of Health P40 OD010440. We acknowledge WormBase for information resources. This work was supported by National Institutes of Health grants R01 NS035546 to Y.J., R01GM088565 to J.K., and R01 GM049369 to X.F. F.C. is an associate and Y. J. is an investigator of the Howard Hughes Medical Institute.

References

Ahn SH, Kim M, Buratowski S. 2004. Phosphorylation of serine 2 within the RNA polymerase II C-terminal domain couples transcription and 3′ end processing. *Mol Cell* **13:** 67–76.

Bataille AR, Jeronimo C, Jacques PE, Laramee L, Fortin ME, Forest A, Bergeron M, Hanes SD, Robert F. 2012. A universal RNA polymerase II CTD cycle is orchestrated by complex interplays between kinase, phosphatase, and isomerase enzymes along genes. *Mol Cell* **45:** 158–170.

Berg MG, Singh LN, Younis I, Liu Q, Pinto AM, Kaida D, Zhang Z, Cho S, Sherrill-Mix S, Wan L, et al. 2012. U1 snRNP determines mRNA length and regulates isoform expression. *Cell* **150:** 53–64.

Boontrakulpoontawee P, Otsuka AJ. 2002. Mutational analysis of the *Caenorhabditis elegans* ankyrin gene *unc-44* demonstrates that the large spliceoform is critical for neural development. *Mol Genet Genomics* **267:** 291–302.

Brenner S. 1974. The genetics of *Caenorhabditis elegans*. *Genetics* **77:** 71–94.

Buratowski S. 2009. Progression through the RNA polymerase II CTD cycle. *Mol Cell* **36:** 541–546.

Chan SL, Huppertz I, Yao C, Weng L, Moresco JJ, Yates JR III, Ule J, Manley JL, Shi Y. 2014. CPSF30 and Wdr33 directly bind to AAUAAA in mammalian mRNA 3′ processing. *Genes Dev* **28:** 2370–2380.

Chen Y, Zhang L, Estaras C, Choi SH, Moreno L Jr, Karn J, Moresco JJ, Yates JR III, Jones KA. 2014. A gene-specific role for the Ssu72 RNAPII CTD phosphatase in HIV-1 Tat transactivation. *Genes Dev* **28:** 2261–2275.

Cheng C, Sharp PA. 2003. RNA polymerase II accumulation in the promoter-proximal region of the dihydrofolate reductase and γ-actin genes. *Mol Cell Biol* **23:** 1961–1967.

Colgan DF, Manley JL. 1997. Mechanism and regulation of mRNA polyadenylation. *Genes Dev* **11:** 2755–2766.

Cui M, Allen MA, Larsen A, Macmorris M, Han M, Blumenthal T. 2008. Genes involved in pre-mRNA 3′-end formation and transcription termination revealed by a lin-15 operon Muv suppressor screen. *Proc Natl Acad Sci* **105:** 16665–16670.

Cunha SR, Mohler PJ. 2009. Ankyrin protein networks in membrane formation and stabilization. *J Cell Mol Med* **13:** 4364–4376.

Davidson L, Muniz L, West S. 2014. 3′ end formation of pre-mRNA and phosphorylation of Ser2 on the RNA polymerase II CTD are reciprocally coupled in human cells. *Genes Dev* **28:** 342–356.

Dichtl B, Blank D, Ohnacker M, Friedlein A, Roeder D, Langen H, Keller W. 2002. A role for SSU72 in balancing RNA polymerase II transcription elongation and termination. *Mol Cell* **10:** 1139–1150.

Dickinson DJ, Ward JD, Reiner DJ, Goldstein B. 2013. Engineering the *Caenorhabditis elegans* genome using Cas9-triggered homologous recombination. *Nat Methods* **10:** 1028–1034.

Di Giammartino DC, Nishida K, Manley JL. 2011. Mechanisms and consequences of alternative polyadenylation. *Mol Cell* **43:** 853–866.

Egloff S, Murphy S. 2008. Cracking the RNA polymerase II CTD code. *Trends Genet* **24:** 280–288.

Elkon R, Ugalde AP, Agami R. 2013. Alternative cleavage and polyadenylation: extent, regulation and function. *Nat Rev Genet* **14:** 496–506.

Flavell SW, Kim TK, Gray JM, Harmin DA, Hemberg M, Hong EJ, Markenscoff-Papadimitriou E, Bear DM, Greenberg ME. 2008. Genome-wide analysis of MEF2 transcriptional program reveals synaptic target genes and neuronal activity-dependent polyadenylation site selection. *Neuron* **60:** 1022–1038.

Frokjaer-Jensen C, Davis MW, Hopkins CE, Newman BJ, Thummel JM, Olesen SP, Grunnet M, Jorgensen EM. 2008. Single-copy insertion of transgenes in *Caenorhabditis elegans*. *Nat Genet* **40:** 1375–1383.

He X, Khan AU, Cheng H, Pappas DL Jr, Hampsey M, Moore CL. 2003. Functional interactions between the transcription and mRNA 3′ end processing machineries mediated by Ssu72 and Sub1. *Genes Dev* **17:** 1030–1042.

Hilgers V, Lemke SB, Levine M. 2012. ELAV mediates 3′ UTR extension in the *Drosophila* nervous system. *Genes Dev* **26:** 2259–2264.

Hirose Y, Manley JL. 1998. RNA polymerase II is an essential mRNA polyadenylation factor. *Nature* **395:** 93–96.

Hsin JP, Sheth A, Manley JL. 2011. RNAP II CTD phosphorylated on threonine-4 is required for histone mRNA 3′ end processing. *Science* **334:** 683–686.

Jenal M, Elkon R, Loayza-Puch F, van Haaften G, Kuhn U, Menzies FM, Oude Vrielink JA, Bos AJ, Drost J, Rooijers K, et al. 2012. The poly(A)-binding protein nuclear 1 suppresses alternative cleavage and polyadenylation sites. *Cell* **149:** 538–553.

Kaida D, Berg MG, Younis I, Kasim M, Singh LN, Wan L, Dreyfuss G. 2010. U1 snRNP protects pre-mRNAs from premature cleavage and polyadenylation. *Nature* **468:** 664–668.

Kim M, Krogan NJ, Vasiljeva L, Rando OJ, Nedea E, Greenblatt JF, Buratowski S. 2004. The yeast Rat1 exonuclease promotes transcription termination by RNA polymerase II. *Nature* **432:** 517–522.

Kim H, Erickson B, Luo W, Seward D, Graber JH, Pollock DD, Megee PC, Bentley DL. 2010a. Gene-specific RNA polymerase II phosphorylation and the CTD code. *Nat Struct Mol Biol* **17:** 1279–1286.

Kim S, Yamamoto J, Chen Y, Aida M, Wada T, Handa H, Yamaguchi Y. 2010b. Evidence that cleavage factor Im is a heterotetrameric protein complex controlling alternative polyadenylation. *Genes Cells* **15:** 1003–1013.

Kolev NG, Yario TA, Benson E, Steitz JA. 2008. Conserved motifs in both CPSF73 and CPSF100 are required to assemble the active endonuclease for histone mRNA 3′-end maturation. *EMBO Rep* **9:** 1013–1018.

Komarnitsky P, Cho EJ, Buratowski S. 2000. Different phosphorylated forms of RNA polymerase II and associated mRNA processing factors during transcription. *Genes Dev* **14:** 2452–2460.

Krishnamurthy S, He X, Reyes-Reyes M, Moore C, Hampsey M. 2004. Ssu72 Is an RNA polymerase II CTD phosphatase. *Mol Cell* **14:** 387–394.

Lianoglou S, Garg V, Yang JL, Leslie CS, Mayr C. 2013. Ubiquitously transcribed genes use alternative polyadenylation to achieve tissue-specific expression. *Genes Dev* **27:** 2380–2396.

Licatalosi DD, Geiger G, Minet M, Schroeder S, Cilli K, McNeil JB, Bentley DL. 2002. Functional interaction of yeast pre-mRNA 3′ end processing factors with RNA polymerase II. *Mol Cell* **9:** 1101–1111.

Licatalosi DD, Mele A, Fak JJ, Ule J, Kayikci M, Chi SW, Clark TA, Schweitzer AC, Blume JE, Wang X, et al. 2008. HITS-CLIP yields genome-wide insights into brain alternative RNA processing. *Nature* **456:** 464–469.

Mangone M, Manoharan AP, Thierry-Mieg D, Thierry-Mieg J, Han T, Mackowiak SD, Mis E, Zegar C, Gutwein MR, Khivansara V, et al. 2010. The landscape of *C. elegans* 3′UTRs. *Science* **329:** 432–435.

Martin G, Gruber AR, Keller W, Zavolan M. 2012. Genome-wide analysis of pre-mRNA 3′ end processing reveals a decisive role of human cleavage factor I in the regulation of 3′ UTR length. *Cell Rep* **1:** 753–763.

Martinson HG. 2011. An active role for splicing in 3′-end formation. *Wiley Interdiscip Rev RNA* **2:** 459–470.

Masamha CP, Xia Z, Yang J, Albrecht TR, Li M, Shyu AB, Li W, Wagner EJ. 2014. CFIm25 links alternative polyadenylation to glioblastoma tumour suppression. *Nature* **510:** 412–416.

Mayr C, Bartel DP. 2009. Widespread shortening of 3′UTRs by alternative cleavage and polyadenylation activates oncogenes in cancer cells. *Cell* **138:** 673–684.

McCracken S, Fong N, Yankulov K, Ballantyne S, Pan G, Greenblatt J, Patterson SD, Wickens M, Bentley DL. 1997. The C-terminal domain of RNA polymerase II couples mRNA processing to transcription. *Nature* **385:** 357–361.

Meinhart A, Cramer P. 2004. Recognition of RNA polymerase II carboxy-terminal domain by 3′-RNA-processing factors. *Nature* **430:** 223–226.

Meinhart A, Kamenski T, Hoeppner S, Baumli S, Cramer P. 2005. A structural perspective of CTD function. *Genes Dev* **19:** 1401–1415.

Mello CC, Kramer JM, Stinchcomb D, Ambros V. 1991. Efficient gene transfer in *C.elegans*: extrachromosomal maintenance and integration of transforming sequences. *EMBO J* **10:** 3959–3970.

Millevoi S, Vagner S. 2010. Molecular mechanisms of eukaryotic pre-mRNA 3′ end processing regulation. *Nucleic Acids Res* **38:** 2757–2774.

Misra A, Ou J, Zhu LJ, Green MR. 2015. Global promotion of alternative internal exon usage by mRNA 3′ end formation factors. *Mol Cell* **58:** 819–831.

Mukhopadhyay A, Deplancke B, Walhout AJ, Tissenbaum HA. 2008. Chromatin immunoprecipitation (ChIP) coupled to detection by quantitative real-time PCR to study transcription factor binding to DNA in *Caenorhabditis elegans*. *Nat Protoc* **3:** 698–709.

Nag A, Narsinh K, Martinson HG. 2007. The poly(A)-dependent transcriptional pause is mediated by CPSF acting on the body of the polymerase. *Nat Struct Mol Biol* **14:** 662–669.

Nakata K, Abrams B, Grill B, Goncharov A, Huang X, Chisholm AD, Jin Y. 2005. Regulation of a DLK-1 and p38 MAP kinase pathway by the ubiquitin ligase RPM-1 is required for presynaptic development. *Cell* **120:** 407–420.

Otsuka AJ, Boontrakulpoontawee P, Rebeiz N, Domanus M, Otsuka D, Velamparampil N, Chan S, Vande Wyngaerde M, Campagna S, Cox A. 2002. Novel UNC-44 AO13 ankyrin is required for axonal guidance in *C. elegans*, contains six highly repetitive STEP blocks separated by seven potential transmembrane domains, and is localized to neuronal processes and the periphery of neural cell bodies. *J Neurobiol* **50:** 333–349.

Phatnani HP, Greenleaf AL. 2006. Phosphorylation and functions of the RNA polymerase II CTD. *Genes Dev* **20:** 2922–2936.

Proudfoot NJ. 2011. Ending the message: poly(A) signals then and now. *Genes Dev* **25:** 1770–1782.

Reyes-Reyes M, Hampsey M. 2007. Role for the Ssu72 C-terminal domain phosphatase in RNA polymerase II transcription elongation. *Mol Cell Biol* **27:** 926–936.

Sandberg R, Neilson JR, Sarma A, Sharp PA, Burge CB. 2008. Proliferating cells express mRNAs with shortened 3′ untranslated regions and fewer microRNA target sites. *Science* **320:** 1643–1647.

Schonemann L, Kuhn U, Martin G, Schafer P, Gruber AR, Keller W, Zavolan M, Wahle E. 2014. Reconstitution of CPSF active in polyadenylation: recognition of the polyadenylation signal by WDR33. *Genes Dev* **28:** 2381–2393.

Shi Y, Di Giammartino DC, Taylor D, Sarkeshik A, Rice WJ, Yates JR III, Frank J, Manley JL. 2009. Molecular architecture of the human pre-mRNA 3′ processing complex. *Mol Cell* **33:** 365–376.

Steinmetz EJ, Brow DA. 2003. Ssu72 protein mediates both poly (A)-coupled and poly(A)-independent termination of RNA polymerase II transcription. *Mol Cell Biol* **23:** 6339–6349.

St-Pierre B, Liu X, Kha LC, Zhu X, Ryan O, Jiang Z, Zacksenhaus E. 2005. Conserved and specific functions of mammalian ssu72. *Nucleic Acids Res* **33:** 464–477.

Sullivan KD, Steiniger M, Marzluff WF. 2009. A core complex of CPSF73, CPSF100, and Symplekin may form two different cleavage factors for processing of poly(A) and histone mRNAs. *Mol Cell* **34:** 322–332.

Sun ZW, Hampsey M. 1996. Synthetic enhancement of a TFIIB defect by a mutation in SSU72, an essential yeast gene encoding a novel protein that affects transcription start site selection in vivo. *Mol Cell Biol* **16:** 1557–1566.

Takagaki Y, Seipelt RL, Peterson ML, Manley JL. 1996. The polyadenylation factor CstF-64 regulates alternative processing of IgM heavy chain pre-mRNA during B cell differentiation. *Cell* **87:** 941–952.

Tian B, Hu J, Zhang H, Lutz CS. 2005. A large-scale analysis of mRNA polyadenylation of human and mouse genes. *Nucleic Acids Res* **33:** 201–212.

Van Epps H, Dai Y, Qi Y, Goncharov A, Jin Y. 2010. Nuclear pre-mRNA 3′-end processing regulates synapse and axon development in *C. elegans*. *Development* **137:** 2237–2250.

Vasiljeva L, Kim M, Mutschler H, Buratowski S, Meinhart A. 2008. The Nrd1–Nab3–Sen1 termination complex interacts with the Ser5-phosphorylated RNA polymerase II C-terminal domain. *Nat Struct Mol Biol* **15:** 795–804.

Wallenfang MR, Seydoux G. 2002. *cdk-7* is required for mRNA transcription and cell cycle progression in *Caenorhabditis elegans* embryos. *Proc Natl Acad Sci* **99:** 5527–5532.

Xiang K, Nagaike T, Xiang S, Kilic T, Beh MM, Manley JL, Tong L. 2010. Crystal structure of the human symplekin–Ssu72–CTD phosphopeptide complex. *Nature* **467:** 729–733.

Xiang K, Manley JL, Tong L. 2012. An unexpected binding mode for a Pol II CTD peptide phosphorylated at Ser7 in the active site of the CTD phosphatase Ssu72. *Genes Dev* **26:** 2265–2270.

Yan D, Jin Y. 2012. Regulation of DLK-1 kinase activity by calcium-mediated dissociation from an inhibitory isoform. *Neuron* **76:** 534–548.

Zhang DW, Mosley AL, Ramisetty SR, Rodriguez-Molina JB, Washburn MP, Ansari AZ. 2012. Ssu72 phosphatase-dependent erasure of phospho-Ser7 marks on the RNA polymerase II C-terminal domain is essential for viability and transcription termination. *J Biol Chem* **287:** 8541–8551.